

# Supplementary Material for Bismuth Ferrite Dielectric Nanoparticles Excited at Telecom Wavelengths as Multicolor Sources by Second, Third, and Fourth Harmonic Generation

Jérémy Riporto,<sup>†,‡</sup> Alexis Demierre,<sup>†</sup> Vasyl Kilin,<sup>†</sup> Tadas Balciunas,<sup>†,¶</sup> Cédric Schmidt,<sup>†</sup> Gabriel Campargue,<sup>†</sup> Mathias Urbain,<sup>‡</sup> Andrius Baltuska,<sup>¶</sup> Ronan Le Dantec,<sup>‡</sup> Jean-Pierre Wolf,<sup>†</sup> Yannick Mugnier,<sup>‡</sup> and Luigi Bonacina<sup>\*,†</sup>

*Applied Physics Department, Université de Genève, 22 chemin de Pinchat, 1211 Genève 4, Switzerland, Université Savoie Mont Blanc, SYMME, F-74000 Annecy, France, and Photonics Institute, TU Wien, Gusshausstrasse 27/E387, 1040, Vienna, Austria*

E-mail: luigi.bonacina@unige.ch

## BFO HNPs characterization

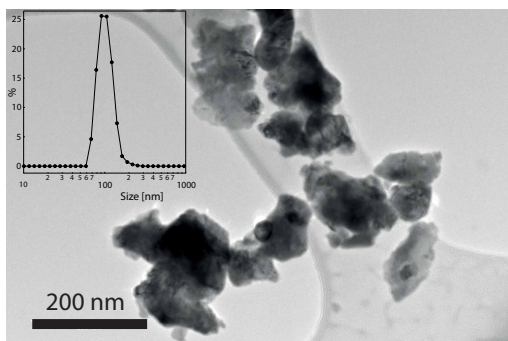


Figure 1: TEM image of BFO HNPs and plot of the Dynamic Light Scattering distribution by number.

A detailed description of the synthesis and properties of the nanoparticles used in this work can be found in Schwung *et al.*,<sup>1</sup> TEM and DLS representative data of a sample obtained by this protocol

<sup>\*</sup>To whom correspondence should be addressed

<sup>†</sup>Applied Physics Department, Université de Genève, 22 chemin de Pinchat, 1211 Genève 4, Switzerland

<sup>‡</sup>Université Savoie Mont Blanc, SYMME, F-74000 Annecy, France

<sup>¶</sup>Photonics Institute, TU Wien, Gusshausstrasse 27/E387, 1040, Vienna, Austria

are reported in Fig. 1.

## Width of the Point Spread Function (PSF) at the different harmonic orders

Taking into account excitation wavelength and objective numerical aperture, the nominal lateral FWHM of a perfect imaging system under linear excitation should be  $\text{FWHM}_{\text{linear}}^{\text{theo}} = 0.51\lambda/\text{N.A.} = 612 \text{ nm}$ .<sup>2</sup> For the non-linear case, Zipfel *et al.* provide the following expression for a two-photon excited fluorescence emitter:  $\text{FWHM}_{\text{2nd order}}^{\text{theo}} = 2\sqrt{\ln 2} \frac{0.325\lambda}{\sqrt{2\text{N.A.}^{0.91}}} = 391 \text{ nm}$ .<sup>3</sup> These values cannot be applied here because the resolution is expected to be severely reduced by the fact that we are using a high N.A. oil immersion objective intended for the visible region and not for an excitation at 1.5  $\mu\text{m}$ . Therefore all aberration corrections and optical elements (comprising the matching medium) are far from optimal. Indeed, we observe an energy reduction of 75% upon laser transmission through this objective, indicating a poor compatibility at this wavelength. By considering that the reso-

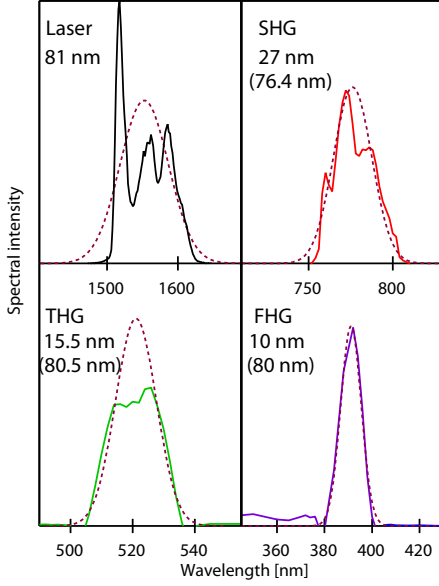


Figure 2: Normalized spectra of laser and different harmonics (continuous lines) along with Gaussian curves supported by the spectra (dashed lines).

lution should be proportional to  $1/\sqrt{n}$  where  $n$  is the nonlinear order, we can readily compute an actual value of  $\approx 840$  nm for the width of the linear PSF, both by multiplying the  $\text{FWHM}_{\text{FHG}}$  (420 nm) by  $\sqrt{4}$  and  $\text{FWHM}_{\text{THG}}$  (486 nm) by  $\sqrt{3}$ . Note that this result supports the fact that we are observing a sub-diffraction limited emitter at two harmonic orders. The same calculation applied to the  $\text{FWHM}_{\text{SHG}}$  (673 nm) provides a result  $\approx 15\%$  higher. In this series, SHG was epi-detected using the *H7421-50* photon counting and THG and FHG forward detected by the *H7732-01* low noise side-on photomultiplier tube. The 15% discrepancy can very likely be attributed to the deviation from linear response of the former detector in the intensity regime of the measurement.

Note that the FWHM value of 840 nm was used for the microscopy-based intensity ratio calculation.

## Estimation of the widths of the harmonic spectra

In Fig. 2, we report the normalized spectra of the laser and of the three harmonics generated by a single BFO HNP along with Gaussian curves supported by these spectra and determined by vi-

sual inspection. On the figure we provide the Gaussian FWHM and, in parentheses, the product  $\text{FWHM} \cdot n\sqrt{n}$  which should be directly compared with the laser spectrum as discussed in the main text.

## Calculation of coherent lengths at different orders

The coherence length is estimated using

$$l_c^{(n)} = \frac{\pi}{k(n\omega) - nk(\omega) - n\Delta k_G} \quad (1)$$

where  $n = 2, 3, 4$  for SHG, THG, and FHG, respectively.  $\Delta k_G$  is the wave vector corresponding to the Gouy-phase shift. The numerical value of  $\Delta k_G$  was estimated at  $-0.5\pi/\lambda$  by Cheng and Xie for a 1.4 N.A. objective.<sup>4</sup>

## Intensity ratios

### Measurements on individual particles

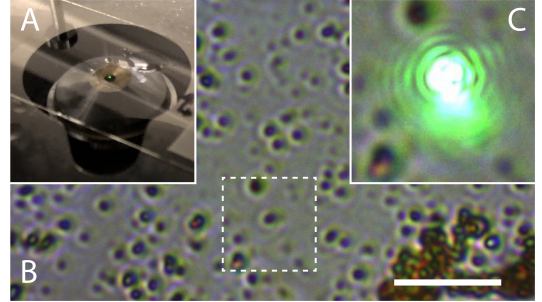


Figure 3: A. Picture of the microscope objective showing the high intensity green (THG) spot generated by a small particle aggregate excited at  $590 \text{ GW/cm}^2$ , visible by naked eye. B. Wide-field transmission image of the sample showing the particle aggregates, the dashed square indicates the object in the laser focus in panel A. C. Close up of the region of the dashed square in B with femtosecond laser ON, showing the strong green emission from the aggregate. Images in A taken using a mobile phone, images in B and C acquired in epi-detection by a compact color CMOS camera (DCC 1645C, Thorlabs - 250 ms integration time). Scale bar  $5 \mu\text{m}$ .

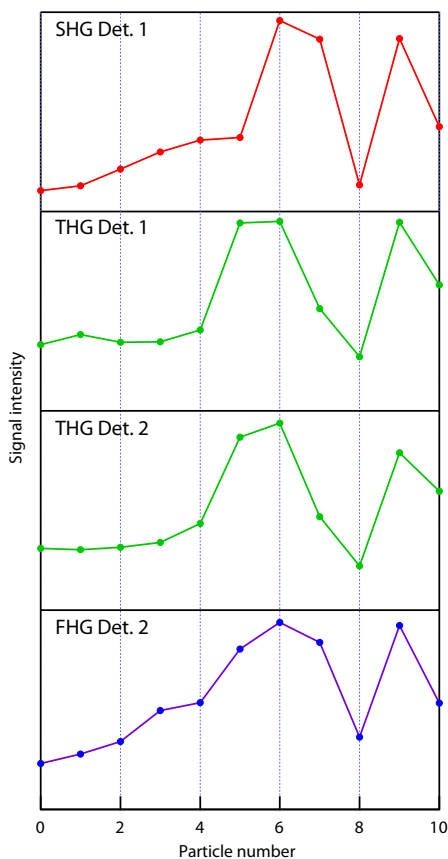


Figure 4: Forward detected signals at the different harmonics generated by 10 distinct HNPs on a microscopy substrate. SHG is measured by detector 1, FHG by detector 2 and THG by both independently.

Intensity ratio measurements by individual BFO HNPs were performed using two different detectors to minimize the need of efficiency corrections among different data sets. As reported in Fig. 4, SHG and THG were measured by detector 1 (SPD-A-VISNIR ultra-low-noise single photon counting module, Aurea Technology) and THG and FHG by detector 2 (H7732-01 low noise sideon photomultiplier tube, Hamamtsu). The traces highlight the particle-to-particle signal intensity variations, which come from differences in sizes (all signals are expected to scale as the particle volume squared), orientations, and possibly varying radiation patterns. We further confirmed these results on magnitude estimation among the different nonlinear orders employing a modified set-up with a NA 0.4 reflective Al-coated objective in the forward arm (Newport) and detecting all harmonics by an EM-CCD (Andor, Ixon3) placed at the imaging output of the spectrometer.

### Ensemble measurements on BFO particle pellets

In Fig. 5A, we provide a SHG image of the BFO HNPs pellet surface obtained by a commercial multiphoton microscope (Nikon A1R-MP) coupled with a Ti:sapphire oscillator (Mai Tai Spectra Physics). The epi-collected signal was processed by a Nikon A1 descanned spectrometer. The image scale bar is  $10\ \mu\text{m}$ . One can see how the SHG intensity of HNPs is modulated by their diverse orientation and that most of the particles appear as bright diffraction limited spots. The emission spectrum averaged over the whole image is reported in Fig. 5B.

For comparing relative intensities of the harmonics on BFO HNPs on dry pellets we relied on the laser set up reported in Fig. 6. This system delivers  $\approx 80$  fs pulses at  $1.5\ \mu\text{m}$  generated in an OPA pumped by a 1 kHz 14 mJ 200-fs Yb:CaF<sub>2</sub> CPA laser. The OPA is based on KTA crystals and seeded by a supercontinuum generated in a bulk YAG plate and delivers 1.5 mJ signal pulses. The signal beam is filtered out at the OPA output using a set of dichroic mirrors, the energy is attenuated using a half-wave plate and a polarizer and then focused onto the sample using  $f=200$  mm CaF<sub>2</sub> lens at  $60^\circ$  incidence. The harmonic sig-

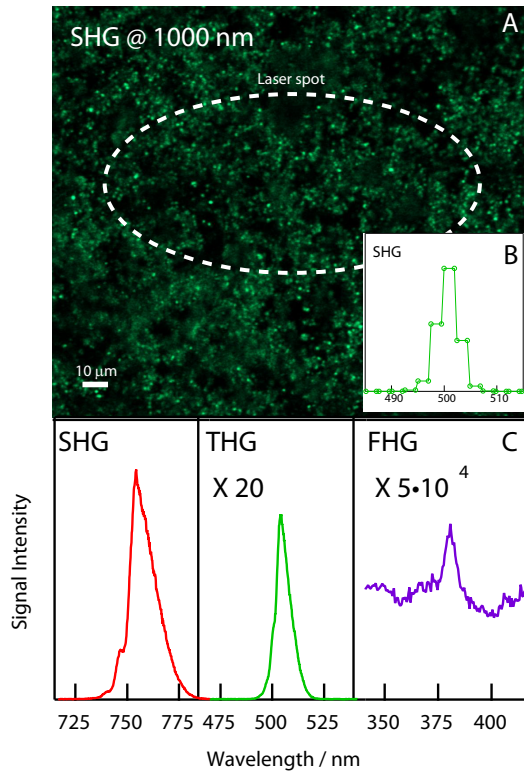


Figure 5: A. SHG image of the surface of BFO HNPs pellet obtained at  $1\mu\text{m}$  excitation. B. SHG spectrum associated to image in A. C. Harmonic spectra generated by the BFO pellet using the KHz laser system tuned at  $1.5\mu\text{m}$ . The relative intensities are corrected for exposition time and spectral properties of the optical components. The dashed line in A indicates the dimension of the focal spot on the sample (at  $\frac{1}{\sqrt{2}}$ ) taking into account the  $60^\circ$  beam incidence.

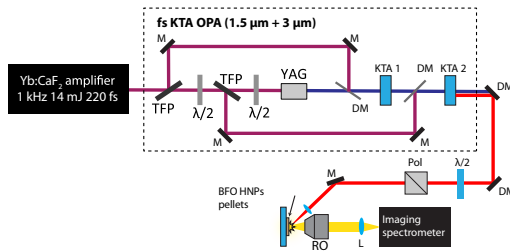


Figure 6: Experimental setup for harmonic generation by BFO HNPs pellets using  $\mu\text{J}$  energy pulses from a femtosecond parametric amplifier. *DM*: dichroic mirror, *TFP*: thin film polarizer, *RO*: reflective objective.

nals are collected in reflection geometry using a Schwarzschild objective (*RefIX*, Edmund Optics), imaged onto the slit of a imaging spectrometer, and detected using an EM-CCD (Andor, Ixon3). In Fig. 4C, we present the spectra of the different harmonic generated by the pellet. The relative intensities are corrected for CCD exposure time and spectral sensitivity and for grating efficiency and can be quantitatively compared.

## References

- (1) Schwung, S.; Rogov, A.; Clarke, G.; Joulaud, C.; Magouroux, T.; Staedler, D.; Passemard, S.; Justel, T.; Badie, L.; Galez, C. *Journal of Applied Physics* **2014**, *116*, 114306.
- (2) Wilson, T. *Journal of microscopy* **2011**, *244*, 113–121.
- (3) Zipfel, W. R.; Williams, R. M.; Webb, W. W. *Nature biotechnology* **2003**, *21*, 1369–1377.
- (4) Cheng, J.-X.; Xie, X. S. *JOSA B* **2002**, *19*, 1604–1610.